

Green Synthesis of Cellulose-Based Biofilms Doped with AgNPs with Antibacterial Activity

Arthur B. D. Pereira,^a Rafael R. A. Silva,^b Clara S. Marques,^b Mayra Aparecida Nascimento,^c Nilda de Fatima F. Soares^b and Renata P. Lopes^{✉*,a}

^aDepartamento de Química, Universidade Federal de Viçosa, 3670-900 Viçosa-MG, Brazil

^bDepartamento de Tecnologia de Alimentos, Universidade Federal de Viçosa, 3670-900 Viçosa-MG, Brazil

^cDepartamento de Engenharia de Materiais, Centro Federal de Educação Tecnológica de Minas Gerais, 30421-169 Belo Horizonte-MG, Brazil

In this work, cellulose-based composite biofilms doped with silver nanoparticles (AgNPs) have been produced by eco-friendly process. The AgNPs were synthesized from *Ilex paraguariensis* with an average size of 45 nm, a characteristic plasmon band at 450 nm and zeta potential of -23 mV. The biofilm has been synthesized by casting method, using different volumes of AgNPs suspension with glycerol plasticizing agent (T6-T10) or not (T1-T5). The AgNPs were successfully incorporated into the biofilms, which was confirmed by scanning electron microscopy. The mechanical and optical structural and the antimicrobial properties of the biofilms have been determined. In the presence of AgNPs, the mechanical properties, thermal stability and water vapor barrier of the biofilms have not been altered. However, the addition of glycerol decreased the tensile strength and the modulus of elasticity, in addition to increasing the elongation of the biofilms and the water vapor barrier. The biofilm T10 showed a transmittance of ca. 10%, with high potential to be used as a UV light blocker. Finally, the biofilms doped with AgNPs showed activity against the bacterium *Pseudomonas fluorescens*. Given the above, this work presented a new biofilm with activity against the bacterium *Pseudomonas fluorescens* obtained by eco-friendly process.

Keywords: green chemistry, sustainability, nanotechnology, eco-friendly, *Pseudomonas fluorescens*

Introduction

Since its development, plastic has been used on a large scale, replacing materials such as metal and glass. This occurs due to its properties such as versatility for different applications, density and mainly, low production cost.^{1,2} One of the most important applications has been directed in the packaging sector,³ adding economy and practicality to the one. Packaging has become essential for human life,³ being found in several sectors. Currently, most packaging is manufactured using conventional plastic. However, the large production of this material resulted in serious environmental problems due to its low degradability.⁴ For example, polyethylene terephthalate (PET) takes about 200 years to be degrade.⁴ Due to the environmental problems caused by the use of plastic from non-renewable sources,

the eco-friendly has emerged as an important component for sustainable economic development.⁵

There is a huge need to replace conventional plastic for others from renewable sources.⁶ The use of biopolymers is an excellent alternative, since they have a shorter degradability time with a half-life time of six months.¹ In this context, cellulose and its derivatives have stood out due to high availability.⁷ In many sectors, besides more sustainable packaging, it is of great interest that packaging can inhibit microbial contamination of packaged products. The food sector is an example, which aims to offer to consumers safer and healthier foods. In this context, the incorporation of silver nanoparticles (AgNPs) into packaging is a promising alternative, since AgNPs have antimicrobial activity.⁸⁻¹¹

At low concentrations, the AgNPs are non-toxic to the human body, which allows them to be used in food packaging.¹² In addition, the silver nanoparticles diffusion to food may not occur or occur at very low concentrations,

*e-mail: renata.plopes@ufv.br

Editor handled this article: Izaura C. N. Diógenes (Associate)

as reported by Zhao *et al.*¹³ According to the authors, the silver has not been detected in the chicken and orange samples after the removal of packages doped with AgNPs. In addition to the antimicrobial action, AgNPs can improve properties such as tensile strength, elastic modulus, tensile breaking stress, UV-barrier and thermal properties of packaging.^{12,14,15} Given the AgNPs use advantages, several works report the incorporation of these nanomaterials in many films applied as antibacterial food packaging, obtaining satisfactory results. Liu *et al.*¹² produced soluble soybean polysaccharide films for preservation of green grapes. Kumar *et al.*¹⁶ produced film consisting of chitosan, gelatin and polyethylene glycol for application in red grapes. Ortega *et al.*¹⁵ produced starch films to prolong the shelf-life of fresh cheese.

There are several processes for the synthesis of AgNPs being the chemical method the most used. In this process, the silver ions present in the solution are reduced by a chemical reductor agent in the presence of a stabilizer.¹⁵ However, green syntheses development using non-toxic solvents and reagents, that do not harm the environment, has increased in recent years.^{15,17,18} The plant extracts can be used to this purpose due to the presence of flavonoids, terpenoids, alkaloids, proteins, carbohydrates, polyphenols, amino acids, among other components. These compounds can act as reductor and stabilizer agents in the AgNPs synthesis.¹⁹ Several works report the use of extracts obtained from different types of plants for the AgNPs synthesis, such as flower of *Moringa oleifera*,¹⁷ aerial and flowering parts of *Lythrum salicaria*,¹⁸ leaf of *Aesculus hippocastanum*,²⁰ flower of *Musa acuminata colla*,²¹ fruits of *Mimosa elengi*,¹⁶ leaf of *Azadirachta indica*.²² Thus, this work aims to synthesize and characterize cellulose-based biofilms doped with AgNPs with antibacterial activity produced by eco-friendly method using *Ilex paraguasiensis* herb.

Experimental

Reagents and solutions

Silver nitrate (CAS 7761-88-8) and sodium chloride (CAS 7647-14-5) were purchased from Neon (Suzano, Brazil). Potassium chromate (CAS 7789-00-6) was obtained from Merck (Darmstadt, Germany). Methyl cellulose (CAS 9004-67-5) and glycerol (CAS 56-81-5) were purchased from Sigma-Aldrich (Saint Louis, United States). The *Ilex paraguasiensis* herb was obtained from the local market in the Viçosa city, Minas Gerais, Brazil. All solutions were prepared in type 1 water, obtained by a Milli-Q system, Millipore corporation (Burlington, United States).

Escherichia coli, *Staphylococcus aureus*, *Pseudomonas fluorescens* and *Listeria innocua* have been used as the indicators of pathogenic bacteria. Mueller Hinton Agar (MHA) growth medium (Cado Mueller-Hinton, Difco Laboratories, Wayne County, USA) and MH agar (Ágar Mueller-Hinton, MHA; Difco Laboratories, Wayne County, USA) were used as a culture medium.

Synthesis and characterization of AgNPs

The silver nanoparticles were synthesized according to the adapted method described by Silveira *et al.*²³ First, the plant extract was obtained, i.e., 100.0 mg of commercial mate tea was weighed in a beaker, under which 50 mL of type 1 water were added. The mixture was heated at 100 °C for 15 min, filtered through qualitative filter paper and the filtrate had its volume adjusted to 50.00 mL. Next, 50.00 mL of silver nitrate solution (2.00 mmol L⁻¹) was added to plant extract, which was kept under orbital stirring, at room temperature (25 °C) for 3.5 h in the absence of light.

The final suspension was characterized by UV-Vis molecular absorption spectroscopy of Thermo Scientific Evolution Array (Waltham, United States), and a quartz cuvette with a 1 cm optical path. The AgNPs suspension were diluted in type 1 water at the ration 1:10 v/v, and then submitted to analysis. The spectra were obtained in the scanning mode from 200 to 1000 nm.

Dynamic light scattering and zeta potential analyzes were performed on the Zetasizer (NanoZS, Malvern, UK). For analysis, 10 µL of AgNPs suspension were diluted with type 1 water in 10.00 mL flask. Then, 2 mL of the diluted suspension was added to the model DTS-1070 cuvette. The analyzes were performed in triplicate at an angle of 173° at a temperature of 25 °C. The non-negative least squares (NNLS) algorithm was used to determine the size distribution of the materials from the correlation curve.

Synthesis of cellulose-based biofilms doped with AgNPs

The biofilms were synthesized using the adapted casting method.²⁴ Ten different synthesis conditions were performed (T1-T10), varying the water and AgNPs suspension volume, with/without plasticizer, as shown in Table 1. Initially, 4.0 g of polymer methyl cellulose were added to a beaker containing a determined volume of type 1 water at 100 °C. The system was submitted to a constant agitation by 15 min. Then, a determined volume of the AgNPs suspension was added to the system, and, in some cases, the glycerol plasticizing agent was added at the concentration of 15% (m/m) in relation to the polymer mass, as shown in Table 1. The system was shaken again by 10 min.

Table 1. Synthesis conditions of biofilms doped with AgNPs

Without plasticizer				With plasticizer ^d			
Treatment	Water / mL	AgNPs ^b suspension / mL	c ^c (AgNPs) / ($\mu\text{mol m}^{-2}$)	Treatment	Water / mL	AgNPs ^b suspension / mL	c ^c (AgNPs) / ($\mu\text{mol m}^{-2}$)
T1	200	0	0	T6	200	0	0
T2	194	6.00	95.4	T7	194	6.00	95.4
T3	188	12.00	190.8	T8	188	12.00	190.8
T4	182	18.00	286.2	T9	182	18.00	286.2
T5	176	24.00	381.6	T10	176	24.00	381.6

^a15% of glycerol (m/m in relation to the polymer mass); ^btheoretical concentration = 1.00 mmol L⁻¹; ^cconcentration of AgNPs in the biofilms.

The obtained dispersions (T1-T10) were poured onto edged glass plates (34 cm × 18.5 cm) at room temperature (25 °C) for 24 h. Next, the systems were stored at 23 °C and 55% relative humidity for 24 h for solvent evaporation.

Characterization of cellulose-based biofilms doped with AgNPs

The biofilms color was analyzed by colorimeter XE Color Quest Hunter lab (Reston, Virginia, United States). All measured values were made according to the CIELAB scale. Only the b coordinate was discussed, that is, from negative to positive, from blue to yellow. For each biofilm (T1-T10), 5 different points were selected, and rectangular samples were cut (2.5 cm × 15 mm). All analyzes were performed in triplicate.

The transparency of the biofilms was determined using a UV-Vis spectrophotometer (Model UV-18000, Shimadzu Co., Kyoto, Japan) in the scan mode from 200 nm (ultraviolet region) to 800 nm (visible region). The biofilms were cut in a rectangular shape (2.5 cm × 15 mm) and placed on the equipment's film support. For control, the empty support was used, that is, in the absence of biofilm.

The biofilms were analysed by Fourier transform infrared spectroscopy (FTIR) using a spectrometer (Nicolet 6700, Thermo Fisher Scientific Inc., Waltham, MA, United States) equipped with a germanium crystal attenuated total reflectance (ATR) accessory. Approximately 4 cm² of each biofilm was used for the analysis. The spectra were obtained at a resolution of 4 cm⁻¹, with wavenumbers from 4000 to 700 cm⁻¹ and 32 scans were performed for each spectrum.

The thermal decomposition of the biofilms was evaluated by the thermogravimetric method using a thermogravimetric analysis (TGA) analyzer of Shimadzu, model DTG-60H (Kyoto, Japan). Approximately 3 mg of each biofilm was heated to 450 °C at a heating rate of 10 °C min⁻¹ in a nitrogen atmosphere with a flow rate of 50 mL min⁻¹.

The biofilms images were obtained using a scanning electron microscope (SEM) (Hitachi High Technologies

America, model TM3000, Inc. Schaumburg, IL, United States). Approximately 4 cm² of biofilm samples were embedded in graphite adhesive. The electron acceleration voltage used was 15 kV with 400× image magnification. To verify the presence of AgNPs, energy dispersive X-ray spectroscopy (EDS) was used using the silicon drift detector.

The thickness and mechanical properties of the biofilms were determined. For this, 3 biofilms of each treatment (T1-T10) were prepared. Five samples (15 mm × 25 mm) were collected at different points of each biofilm. The thickness was determined using a digital micrometer of Mitutoyo Corporation (Takatsu-ku, Japan), with a precision of 0.001 mm. The measurements were performed at 10 random points for each sample.

Maximum tensile strength, breaking stress and Young's modulus were determined by tensile testing using Universal Mechanical Testing Machine, model 3367 (Instron Corporation, Norwood, MA, United States), equipped with a 500 N load cell. The analysis was performed according to ASTM D883-12.²⁵

The water vapor barrier of biofilms was determined using the desiccant method, according to adapted ASTM E96/E96M method.²⁶ The biofilms were cut into 80.0 mm diameter samples and were placed under the circular paraffin capsules, numbered, and sealed with liquid paraffin. A saturated solution of MgCl₂ was used inside the capsules, reaching 33% relative humidity. Then, these biofilms were stored in a desiccator containing a saturated solution of NaCl at 76% relative humidity, with a final relative humidity of 43%. The samples were weighed every 2 h for 22 h. Water vapor permeability was calculated using three replicates and expressed in (g $\mu\text{m m}^{-2} \text{day}^{-1} \text{kPa}^{-1}$).

Biological assays *in vitro*

The antibacterial activity of the biofilms was investigated against two Gram-positive bacteria (*Staphylococcus aureus*-ATCC 6538 and *Listeria innocua*-ATCC 33090) and two

Gram-negative bacteria (*Escherichia coli*-ATCC 11229 and *Pseudomonas fluorescens*-0A7). The bacteria *S. aureus* and *E. coli* are associated to hygiene conditions by food contamination.²⁷ *L. innocua* is a non-pathogenic microorganism often investigated as a surrogate for *Listeria monocytogenes*, an important foodborne pathogen.²⁸ *P. fluorescens* is a relevant spoilage microorganism in dairy products.²⁹

To obtain the inoculum, the bacteria were activated twice in brain heart infusion broth (BHI, Kasvi, Italy), incubated for 24 h at 23 °C for *P. fluorescens* and 37 °C for the others, streaked over plate count agar (PCA, Oxoid, England) and incubated again at the same conditions. Colonies of each bacterium were selected from PCA and suspended in 0.85% (m/v) saline solution to obtain suspensions similar to 0.5 McFarland turbidity standard (around 1×10^8 colony-forming unit (CFU) mL⁻¹). After, the bacterial suspensions were spread on the dried surface of Mueller Hinton agar (Difco Laboratories, Wayne County, USA) (*E. coli*, *S. aureus*, and *P. fluorescens*) or BHI agar (*L. innocua*) with the aid of a swab, and samples of the manufactured films (diameter = 1 cm) were placed on the agar. The Petri dishes were incubated for 24 h at 37 ± 1 °C or 23 ± 1 °C, and the inhibition zones were measured in mm. The assays were performed in triplicate.

Results and Discussion

The AgNPs were synthesized using yerba mate extract (*Ilex paraguariensis*), whose FTIR spectrum is shown in Figure S1, Supplementary Information (SI) section. As can be seen, the spectrum is quite complex, due to its variety of organic compounds, such as polyphenols and organic acids.^{30,31} The band at 3416 cm⁻¹ can be attributed to the O–H bond stretching, while the bands at 2923 and 2850 cm⁻¹ can be related to the C–H bond stretching. The bands at 1612 cm⁻¹ can be associated to carbonyl groups present in polyphenols and organic acids. The band near 1461 cm⁻¹ can be attributed to the O–C–O stretching, while the band at 1250 cm⁻¹ can be refer to the C–O groups vibration. The band around 830 cm⁻¹ can be attributed to the C–H bond vibration of the polyphenols aromatic rings and organic acids.²³ Therefore, it is possible to verify strong indications of the functional groups presence in the yerba mate, that are responsible for the reduction and colloidal stability of the nanoparticles,³² such as polyphenols and organic acids. Santos *et al.*³³ described that chlorogenic acid, caffeine and flavonoids such as rutin, are the main species responsible for the reduction and stabilization of AgNPs.

The AgNPs formation could be observed macroscopically, since the reaction of the plant extract

with the silver nitrate solution showed an orange-brown color, indicating the nanoparticles formation (inset of Figure 1). The UV-Vis spectra of AgNPs suspensions are shown in Figure 1. The AgNPs is confirmed by the characteristic band around 450 nm. This band occurs due to the phenomenon of surface plasmonic resonance, which occurs with silver nanoparticles of 45 nm in size.³⁴ The size of AgNPs present in the suspension was estimated by dynamic light scattering (DLS) analysis, as can be seen in the Figure S2, SI section. The AgNPs suspension presented two particle size distributions, one centered at 45 nm and the other at 400 nm. This characteristic can be attributed to the polydispersity of the suspension, due the presence nanometer scale particles (< 100 nm) and others of larger size. The particles of approximately 45 nm can be attributed to AgNPs. These results can be confirmed by UV-Vis spectroscopy, whose band at 450 nm refers to particles in this size range. Similar works that used plant extracts to synthesize AgNPs also obtained particle sizes below 100 nm. Alkhulaifi *et al.*³⁵ synthesized AgNPs of 10-25 nm from *Citrus limon* extract. Tailor *et al.*³⁶ synthesized AgNPs of 16 nm from *Ocimum canum* extract. Ponsanti *et al.*³⁷ obtained AgNPs from corn starch with a size of 47.8 nm. Some particles of 100-1000 nm size were also observed with great frequency in the AgNPs suspension (Figure S2). Particles with sizes between 100-1000 nm can be attributed to particles from components present in tea such as polyphenols, polysaccharides, and proteins. These particles form a colloidal system after tea infusion and were previously characterized. Han *et al.*³⁸ identified particles with a hydrodynamic diameter of 128 nm in black tea infusion. Guo *et al.*³⁹ identified particles of 363.8 nm in green tea infusion. Lin *et al.*⁴⁰ observed the presence of particles of 517.4 and 226.1 nm in green tea and black tea infusions, respectively.

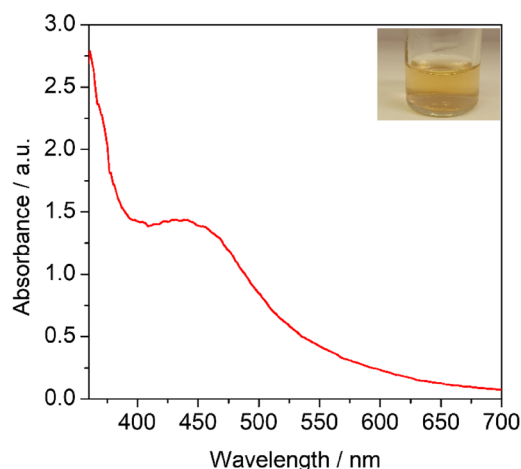


Figure 1. UV-Vis spectra of AgNPs suspensions synthesized by *Ilex paraguariensis* extract. Inset: photo of AgNPs suspension.

The AgNPs suspension presented zeta potential of -23.8 ± 1.2 mV. This result is similar to literature data for AgNPs suspensions obtained from green synthesis. Rolim *et al.*⁴¹ synthesized silver nanoparticles from green tea extract whose suspension presented a zeta potential of -35.5 ± 3.2 mV. Umaí *et al.*⁴² synthesized AgNPs suspension from olive species (*Olea europaea*) with zeta potential of -35 mV. The negative potential indicates that the charge of the double layer on the nanoparticles is negative, that is, negatively charged molecules are stabilizing the AgNPs. However, the value is not very high, which makes the nanoparticle suspension not very stable. For a suspension to be considered stable, it is necessary that its zeta potential is greater than 30 mV, in modulus.⁴³ This is due to the forces of interaction and repulsion between the nanoparticles. The greater magnitude of the zeta potential, the greater stability of the suspension and, therefore, the greater value of electrostatic repulsion.⁴³ Once the AgNPs were characterized, they were used to produce biofilms.

Cellulose-based biofilms doped with AgNPs

After production, the biofilms were packaged, and vacuum sealed for better conservation. The biofilm T10 is shown in Figure S3, SI section. The other biofilms were very similar. The color is one of the most important parameters to produce a package, whose main function is to attract the consumer. The color is evaluated from the parameter b (CIELAB scale), which indicates the yellow color index of the film. Thus, this parameter was determined for each biofilm described in the Table 1, whose results are shown in Figures 2a-2b.

It can be observed that the b coordinate of the biofilms increases with the addition of AgNPs suspension, for biofilms without (Figure 2a) and with plasticizer

(Figure 2b). As the AgNPs suspension was yellow (Figure 1), these results were already expected. The AgNPs coloration in the visible region is due to the surface plasmonic resonance effect of the metallic nanoparticles.

A linear correlation between AgNPs suspension volume and the parameter b can be observed in the Figure S4 (SI section), with adjusted R^2 (determination coefficient) bigger than 0.95, for both conditions with and without plasticizer. This result indicates that when the volume of AgNPs suspension added increases, the parameter b increases in a linear relation. Ortega *et al.*¹⁵ obtained similar results from corn starch film containing AgNPs obtained from maltose solution.

The transparency property is another important parameter in biofilms because the consumers tend to observe the product they want to buy. This parameter was evaluated by UV-Vis spectroscopy, whose results are shown in Figures 3a-3b for biofilms without and with plasticizer. An inflection point is observed in the spectra at 395 nm. As the volume of suspension added increased (T1 to T5 and T6 to T10), there was a lower transmittance value at 395 nm. This transmittance value decreasing indicates that the yellow color of the biofilm is bigger. These results agree with the results obtained by colorimetry once the b coordinate increases with AgNPs suspension volume increase. The glycerol-containing biofilms present lower transmittance (T7-T10) than correspondent biofilms without glycerol (T2-T5), specially at 395 nm. According to Teixeira *et al.*,⁴⁴ a larger opacity of glycerol-containing biofilms can be attributed to the difficulty of the plasticizing agent to disperse in the polymer matrix.

In addition, a small transmittance value ($< 10\%$) in the ultraviolet region (UVA, UVB and UVC, 100-400 nm) and visible region (400-700 nm) ranges indicates that the film presents light blocker characteristics.¹⁵ The biofilm T10

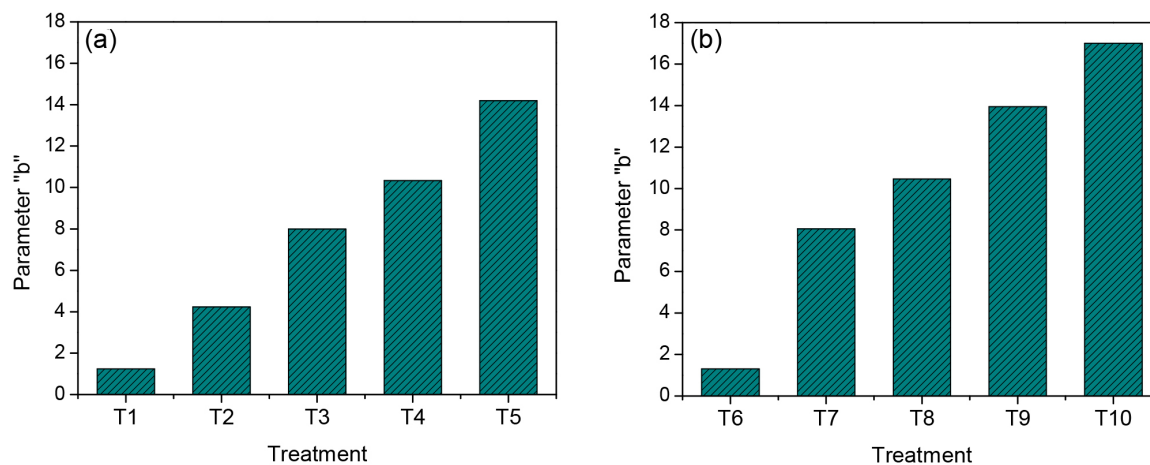


Figure 2. Colorimetric assay performed for biofilms (a) T1-T5 without plasticizer and (b) T6-T10 with plasticizer. T1 and T6: without AgNPs; T2 and T7: $95.4 \mu\text{mol m}^{-2}$ AgNPs; T3 and T8: $190.8 \mu\text{mol m}^{-2}$ AgNPs; T4 and T9: $286.2 \mu\text{mol m}^{-2}$ AgNPs and T5 and T10: $381.6 \mu\text{mol m}^{-2}$ AgNPs.

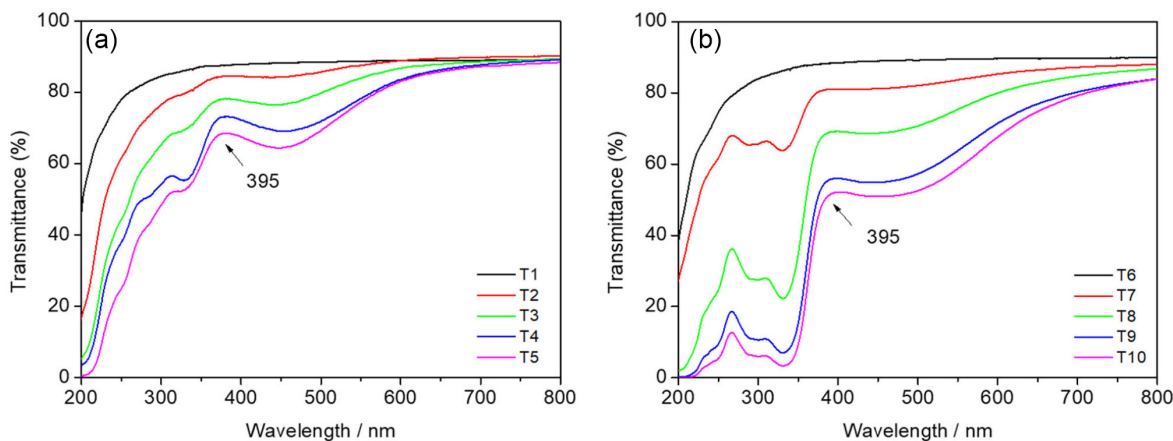


Figure 3. UV-Vis spectra of biofilms doped with AgNPs (a) treatments: T1-T5 without plasticizer (b) treatments: T6-T10 with plasticizer. T1 and T6: without AgNPs; T2 and T7: $95.4 \mu\text{mol m}^{-2}$ AgNPs; T3 and T8: $190.8 \mu\text{mol m}^{-2}$ AgNPs; T4 and T9: $286.2 \mu\text{mol m}^{-2}$ AgNPs and T5 and T10: $381.6 \mu\text{mol m}^{-2}$ AgNPs.

showed a low transmittance value for UVB (220-280 nm) and UVC ranges (280-100 nm). In this way, the T10 biofilm has potential as a light blocker, which is interesting in the food packing sector, since foods tend to be degraded in the light presence.

The biofilms were also characterized by infrared spectroscopy and the results of *Ilex paraguariensis* herb, T1 (without AgNPs) and T5 (with AgNPs) are shown in Figure 4. It is possible to observe that the band at 985 cm^{-1} referring to biopolymer methyl cellulose²⁴ is observed in T1 and T5 biofilms. Bands referring to mate tea,²³ such as 2923, 2850, 2036, 1702, 1461, 1205, 830 cm^{-1} , previously discussed, are present only in T5, because T1 does not contain tea extract (without AgNPs). This result is a strong indication that the tea extract was incorporated into the methyl cellulose biofilms, and probably the AgNPs.

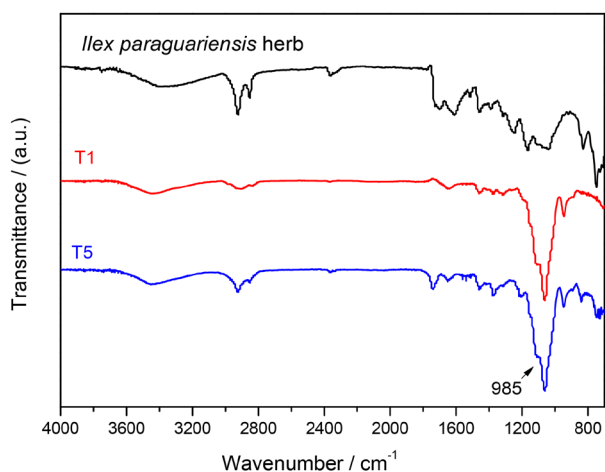


Figure 4. FTIR (ATR) spectrum of the *Ilex paraguariensis* herb, T1 (without AgNPs) and T5 (with AgNPs).

The thermal stability of biofilms was evaluated by thermogravimetry. The results of the T1, T5, T6 and T10 biofilms are shown in Figures 5a-5d. A thermal event can

be observed at about $100 \text{ }^\circ\text{C}$, which occurs for all biofilms. In this event about 10% of matter is lost, which can be attributed to desorption and evaporation of water.⁴⁵ For the T6 and T10 biofilms, a thermal event is observed at $200 \text{ }^\circ\text{C}$. Probably, this mass loss is related to the plasticizing agent, present in these biofilms. The boiling temperature of glycerol is $290 \text{ }^\circ\text{C}$. However, as this substance interacts with the polymeric chains of methyl cellulose and, therefore, its boiling point is reduced,⁴⁶ as can be seen in Figures 5c-5d. Another event, common to all produced biofilms whose results are shown in the Table S1 (SI section), occurs between $341\text{-}361 \text{ }^\circ\text{C}$, which can be attributed to the methyl cellulose degradation. Dicastillo *et al.*⁴⁷ also observed the methyl cellulose degradation at $361 \text{ }^\circ\text{C}$. Therefore, it can be concluded that the AgNPs did not contribute to increase the thermal stability of the biofilms produced.

The biofilms were analyzed by SEM and the images of T1 (without glycerol and without AgNPs), T5 (without glycerol and with AgNPs), T6 (with glycerol and without AgNPs) and T10 (with glycerol and with AgNPs) are shown in Figures 6a-6d. The biofilms presented a homogeneous appearance with few granules, attributed to methyl cellulose, that are highlighted in the images (Figures 6a and 6c). For the biofilms containing AgNPs, small white spots can be seen (Figures 6b and 6d), highlighted in yellow in the images. Therefore, it can be concluded that these spots are possibly due to silver nanoparticles.

In the T5 biofilm, the AgNPs present greater agglomeration and, therefore, can be more easily visualized. However, in the T10 biofilm, due to the presence of glycerol, the AgNPs are more dispersed, being its observation more difficult, except in some points as highlighted in Figure 6d. In general, the biofilms with and without glycerol were very similar, being possible to observe a good dispersion of AgNPs. The distribution of the nanoparticles in polymeric films can influence its properties.⁴² Estrada-Monje *et al.*⁴⁸

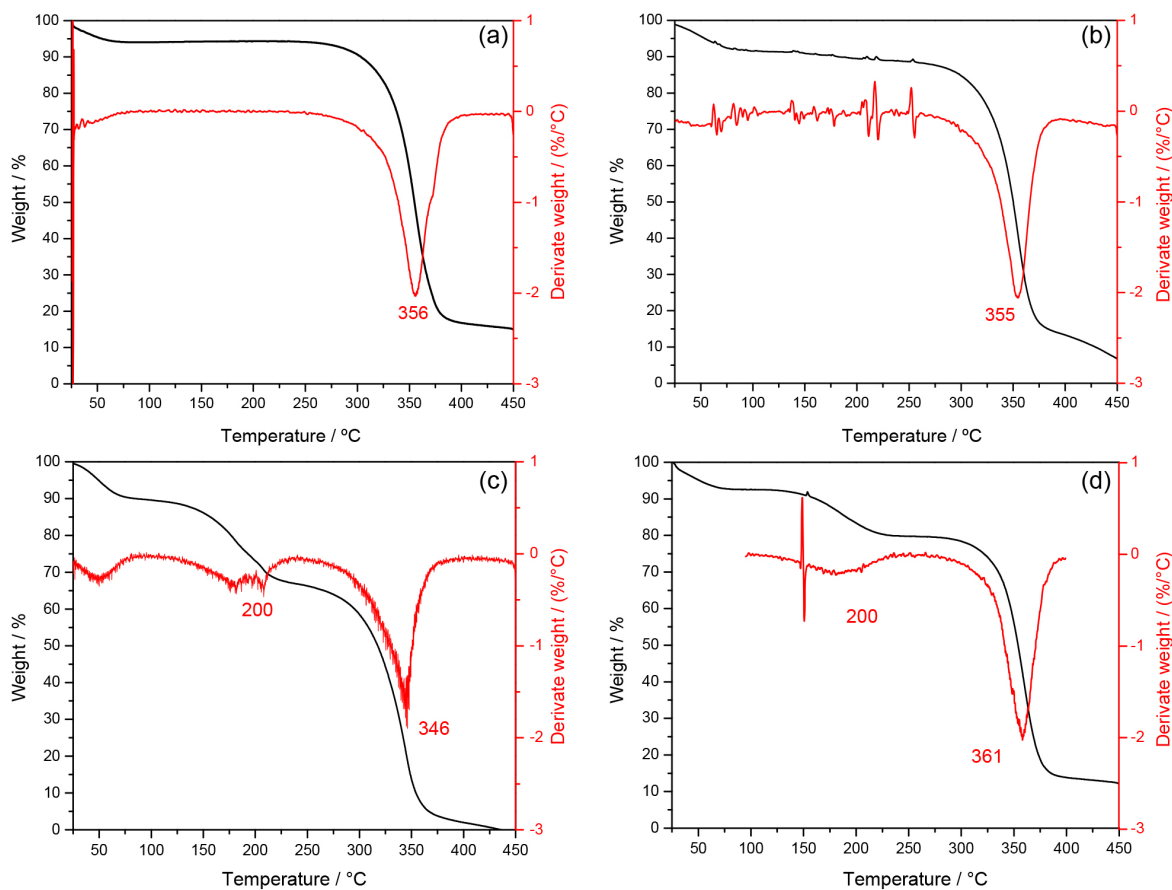


Figure 5. Thermogravimetric curves obtained for treatments T1-without glycerol and AgNPs (a), T5 -without glycerol and with AgNPs ($381.6 \mu\text{mol m}^{-2}$) (b), T6-with glycerol and without AgNPs (c) and T10-with glycerol and AgNPs ($381.6 \mu\text{mol m}^{-2}$) (d).

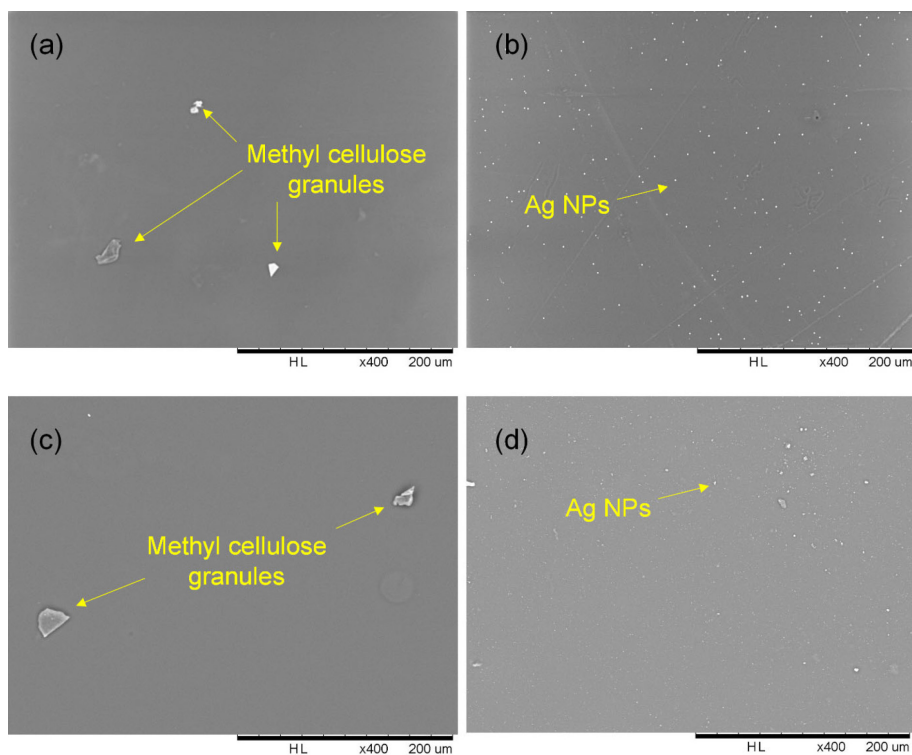


Figure 6. SEM images of cellulose-based biofilms (a) T1: without AgNPs and without glycerol, (b) T5: with AgNPs ($381.6 \mu\text{mol m}^{-2}$) and without glycerol, (c) T6: without AgNPs and with glycerol (d) T10: with AgNPs ($381.6 \mu\text{mol m}^{-2}$) and with glycerol.

evaluated the dispersion of TiO₂ nanoparticles in ethylene-co-vinyl acetate (EVA) films. The authors concluded that the films with more dispersed nanoparticles showed better inhibition efficiency against *Escherichia coli*.

SEM-EDS images of biofilms containing glycerol T6 (without AgNPs), T7 (95.4 $\mu\text{mol m}^{-2}$ of AgNPs) and T10 (190.8 $\mu\text{mol m}^{-2}$ of AgNPs) are shown in Figure S5 (SI section). As T6 does not have AgNPs, only carbon and oxygen mapping are shown in Figure S5a. These elements are homogeneously distributed in the polymer matrix. According to the images, the presence of AgNPs is confirmed, being concluded that the AgNPs were incorporated into the methyl cellulose biopolymer matrix. The energy dispersive X-ray analysis (EDX) analyzes for T7 and T10 biofilms are showed at different scales, 700 and 900 μm , respectively. Although they appear to have the same distribution of AgNPs, the silver concentration in T10 is higher than T7, since more AgNPs suspension was added in T10.

Biofilms thickness values are shown in Table 2. It can be observed that there was no correlation between film thickness and AgNPs suspension volume, obtaining an average thickness of 0.057 and 0.061 mm for biofilms without and with plasticizer, respectively. A Tukey's test was performed for the T1-T5 and T6-T10 biofilms to verify if the AgNPs and the plasticizing agent influence in thickness of the films. According to the result, at the 95% confidence level, all thickness values are equal. Therefore, it can be concluded that the thickness is not influenced by the AgNPs addition and the plasticizer.

The biofilms mechanical properties were characterized by percentage elongation, maximum tensile strength, and modulus of elasticity. The percentage elongation are shown in Figure 7a for biofilms without and with plasticizer. The addition of plasticizer increases considerably the elongation of the biofilms, which has an average value of 18%. This result may be justified due the fact that the plasticizing

Table 2. Thickness values (\pm standard deviation) for biofilms doped with AgNPs

Treatment	Thickness / mm	Treatment	Thickness / mm
T1	0.056 \pm 0.011 ^a	T6	0.060 \pm 0.008 ^a
T2	0.062 \pm 0.019 ^a	T7	0.064 \pm 0.001 ^a
T3	0.060 \pm 0.006 ^a	T8	0.065 \pm 0.001 ^a
T4	0.054 \pm 0.005 ^a	T9	0.056 \pm 0.013 ^a
T5	0.053 \pm 0.019 ^a	T10	0.062 \pm 0.006 ^a

^aGroup belonging to the same statistical treatment, whose values do not differ statistically at the 95% confidence level.

agent increases the distance of one polymeric chain to the other, increasing the elasticity and, consequently, the biofilm can stretch more. The addition of AgNPs did not have a significant effect.

As can be seen in the Figure 7a, the addition of plasticizing agent increased the percentage elongation. The elasticity modulus (Figure 7b) and the maximum tensile strength of the biofilms were also evaluated (Figure S6, SI section). The elasticity modulus can be defined by the ratio of stress that the film has suffered to the tension that a load was applied to the film. The elasticity modulus value consists of the maximum stress value that the film can withstand without undergoing permanent deformation. That is, the elasticity modulus is related to the maximum tensile strength value that the film can withstand when being stretched or pulled. The addition of plasticizing agent (glycerol) decreased the elastic modulus and the maximum tensile strength of biofilms. This phenomenon occurs because the addition of plasticizing agent allows hydrogen bond interactions between the glycerol and the oxygenated groups of the methyl cellulose biopolymer. Therefore, there is less interaction between the biopolymer chains, reducing the resistance and the elastic modulus of the biofilms. Regarding the AgNPs, it was not possible to

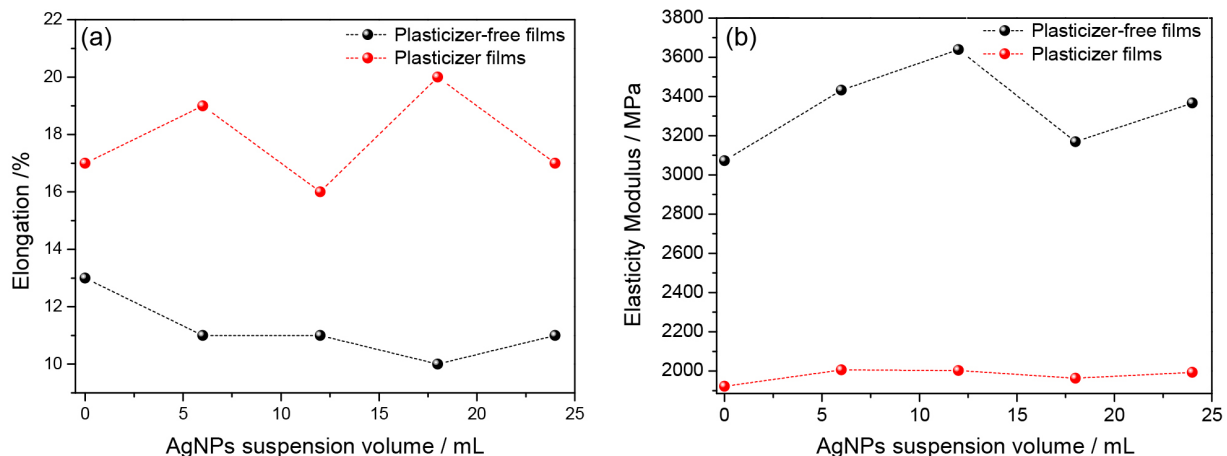


Figure 7. Mechanical properties of biofilms doped with AgNPs (a) percent elongation (b) elastic modulus.

observe any correlation between the parameters evaluated.

The water vapor permeability is one of the main properties of biodegradable films used as food packaging. This parameter defines the application of the biofilm, whether for drier or wetter food packaging. The desiccant method was used for determined this parameter and the results are shown in Table 3.

Table 3. Water vapor permeability (WVP) of biofilms doped with AgNPs

Biofilm/ treatment	WVP ($\times 10^{-13}$) / ($\text{g m m}^{-2} \text{s}^{-1} \text{Pa}^{-1}$)	Biofilm/ treatment	WVP ($\times 10^{-13}$) / ($\text{g m m}^{-2} \text{s}^{-1} \text{Pa}^{-1}$)
T1	5.87	T6	8.51
T2	6.52	T7	6.45
T3	6.91	T8	8.45
T4	6.81	T9	9.11
T5	6.64	T10	9.23

The water vapor permeability (WVP) obtained were higher than synthetic polyethylene films ($1.91 \times 10^{-12} \text{ g m m}^{-2} \text{ s}^{-1} \text{ Pa}^{-1}$).⁴⁹ Roy and Rhim⁵⁰ produced starch/agar films containing AgNPs with WVP of $0.64 \times 10^{-9} \text{ g m m}^{-2} \text{ s}^{-1} \text{ Pa}^{-1}$. Ortega *et al.*¹⁵ produced corn starch-based films containing AgNPs with WVP of $1.9 \times 10^{-10} \text{ g m}^{-1} \text{ s}^{-1} \text{ Pa}^{-1}$. According to the authors, this property extended the shelf life of fresh cheese samples by 21 days. The treatments containing the plasticizing agent (T6-T10) have a higher permeability (6.45×10^{-13} - $9.23 \times 10^{-13} \text{ g m m}^{-2} \text{ s}^{-1} \text{ Pa}^{-1}$), when compared with treatments without plasticizer (T1-T5), whose permeability ranged from 5.87×10^{-13} to $6.91 \times 10^{-13} \text{ g m m}^{-2} \text{ s}^{-1} \text{ Pa}^{-1}$. This phenomenon occurs because the presence of plasticizing

agent moves away the polymer chains and, consequently, the water molecules are more easily absorbed. Therefore, the water vapor permeability value is increased. It is worth mentioning that the methyl cellulose biopolymer is very hydrophilic, that is, it absorbs a lot of water. Thus, it can be concluded that biofilms doped with AgNPs produced in this work are hydrophilic and should be used in drier foods to enable a better application.

Evaluation of the antibacterial activity of biofilms

The antibacterial activity of the synthesized biofilms was evaluated from the halo assay and the results are shown in Figure 8. The biofilms showed microbiological action only for the Gram-negative *P. fluorescens*, showing selectivity for this strain. The halo of inhibition ranging from 1.45 to 1.70 cm, as shown in Table S3 (SI section). For T1 (AgNPs free), the halo of inhibition was zero. An exponential model (adjusted $R = 0.9857$) was fitted to the obtained data for the T1-T5 biofilms (equation 1), whose curve is shown in Figure S7 (SI section). Although has not been observed an inhibition halo against the other microorganisms, these results are promising. *P. fluorescens* is a spoilage bacterium of great importance in the food industry due to its ability to grow under refrigeration.²⁹ It can contaminate several dairy products, causing serious defects, such as the appearance of bluish stains on cheeses, and reducing its shelf life.⁵¹

$$\text{halo} = 1.61 - 1.61e^{-0.36v} \quad (1)$$

wherein v is the AgNPs suspension volume added.

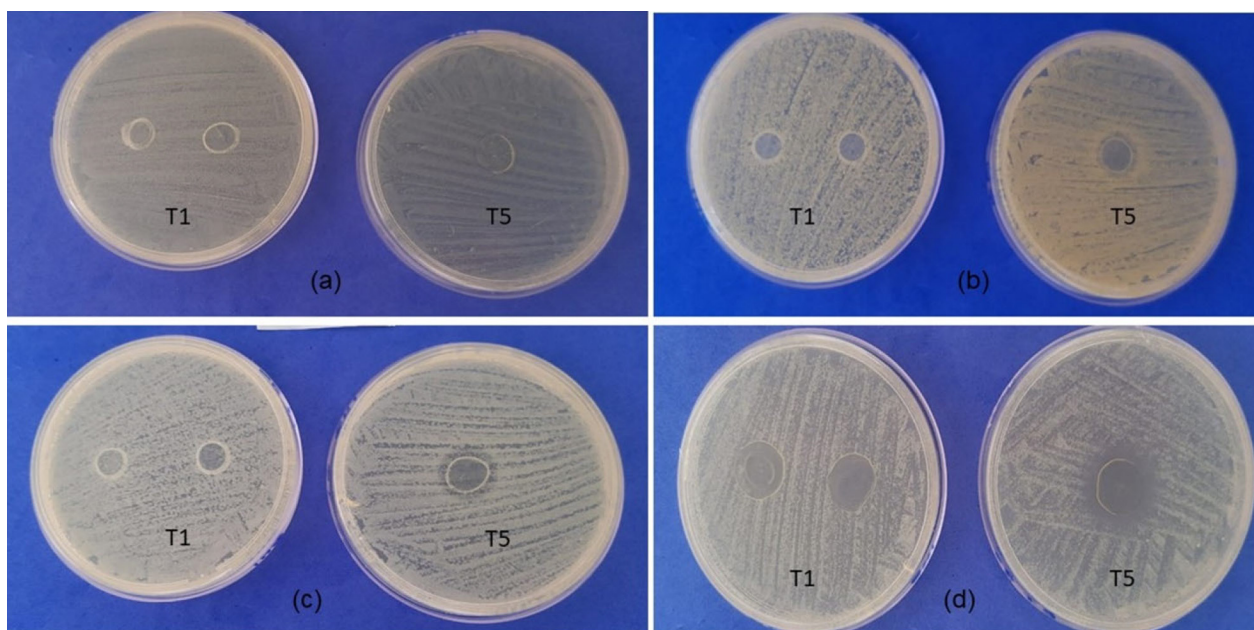


Figure 8. Biological assay for bacteria (a) *Listeria innocua*; (b) *Staphylococcus aureus*; (c) *Escherichia coli*; (d) *Pseudomonas fluorescens* for T1 and T5 films.

The model shows that halo growth is observed only when AgNPs suspension is added to the biofilm. Therefore, the activity is related to the AgNPs and not to the methyl cellulose biopolymer. For biofilms containing glycerol (T6-T10), only the biofilm T10 showed antibacterial activity. This result can be associated to the fact that glycerol is also used as a stabilizing agent for AgNPs. Possibly, the glycerol interacts strongly with silver nanoparticles and prevents them from diffusing into the culture medium, thus decreasing antimicrobial activity. Similar results are found in the literature, in which AgNPs are active against *Pseudomonas aeruginosa*⁵² and *Pseudomonas putida*.⁵³

Conclusions

Thus, it can be concluded that a new composite biofilm based on cellulose doped with AgNPs with potential to be used as antimicrobial packaging was efficiently synthesized. The suspension of silver nanoparticles was synthesized via green synthesis using *Ilex paraguariensis* herb and were successfully incorporated into the biofilm, confirmed by different analytical techniques. AgNPs did not change the mechanical properties of the biofilm, only the plasticizing agent, that is, glycerol. The biofilm containing glycerol and with a higher concentration of AgNPs has the potential to block UV light. In addition, the synthesized biofilms showed activity against the Gram-negative bacterium *Pseudomonas fluorescens*. Finally, this work presented an effective biofilm synthesis based on green chemistry that have high potential to be used as packaging in the food area.

Supplementary Information

Supplementary information is available free of charge at <http://jbcs.sbq.org.br> as PDF file.

Acknowledgments

The authors would like to thank to the Conselho Nacional de Desenvolvimento Científico e Tecnológico (CNPq), Fundação de Amparo à Pesquisa do Estado de Minas Gerais (FAPEMIG), CNPq/FAPEMIG (agreement recorded in SICONV: 793988/2013), Coordenação de Aperfeiçoamento de Pessoal de Nível Superior - Brasil (CAPES) - Finance Code 001.

Author Contributions

Arthur B. D. Pereira was responsible for conceptualization, data curation, formal analysis, investigation, validation, visualization,

writing original draft; Rafael R. A. Silva for conceptualization, formal analysis, investigation, validation, visualization, writing original draft; Clara S. Marques for formal analysis; Mayra Aparecida Nascimento for conceptualization, project administration, writing original draft, writing-review and editing; Nilda de Fatima F. Soares for investigation, project administration, resources; Renata P. Lopes for conceptualization, data curation, formal analysis funding acquisition, project administration, resources, visualization, writing original draft, writing-review and editing.

References

- Landim, A. P. M.; Bernardo, C. O.; Martins, I. B. A.; Francisco, M. R.; Santos, M. B.; de Melo, N. R.; *Polímeros* **2016**, *26*, 82. [Crossref]
- Gad, S. C.; Services, G. C.; *Petroleum Hydrocarbons*, vol. 3, 3rd ed.; Elsevier: Cary, USA, 2014. [Crossref]
- Coelho, M. M. P.; Afonso, A. F.; Trogo, B.; *História da Ciência e Ensino - Construindo Interfaces*, **2017**, *16*, 31. [Crossref]
- Innocentini-Mei, L. H.; Mariani, P. D. S. C.; https://www.feq.unicamp.br/images/stories/documentos/dtp_edps.pdf, accessed in August 2022.
- Provin, A. P.; Dutra, A. R. A.; Gouveia, I. C. A. S. S.; Cubas, A. L. V.; *Technol. Forecast. Soc. Changes* **2021**, *169*, 120858. [Crossref]
- Robaina, M.; Murillo, K.; Rocha, E.; Villar, J.; *Sci. Total Environ.* **2020**, *730*, 139038. [Crossref]
- Ojijo, V.; Sinha Ray, S.; *Prog. Polym. Sci.* **2013**, *38*, 1543. [Crossref]
- Mathew, S.; Snigdha, S.; Mathew, J.; Radhakrishnan, E. K.; *Food Packag. Shelf Life* **2019**, *19*, 155. [Crossref]
- Chawla, R.; Sivakumar, S.; Kaur, H.; *Carbohydr. Polym. Technol. Appl.* **2021**, *2*, 100024. [Crossref]
- Peighambari, S. J.; Peighambari, S. H.; Pournasir, N.; Pakdel, P. M.; *Food Packag. Shelf Life* **2019**, *22*, 100420. [Crossref]
- Carbone, M.; Donia, D. T.; Sabbatella, G.; Antiochia, R.; *J. King Saud Univ., Sci.* **2016**, *28*, 273. [Crossref]
- Liu, J.; Ma, Z.; Liu, Y.; Zheng, X.; Pei, Y.; Tang, K.; *Food Packag. Shelf Life* **2022**, *31*, 100800. [Crossref]
- Zhao, X.; Wang, K.; Ai, C.; Yan, L.; Jiang, C.; Shi, J.; *Food Packag. Shelf Life* **2021**, *28*, 100669. [Crossref]
- Zhang, J.; Cao, C.; Wang, Y.; Xie, L.; Li, W.; Li, B.; Guo, R.; Yan, H.; *Food Packag. Shelf Life* **2021**, *30*, 100748. [Crossref]
- Ortega, F.; Giannuzzi, L.; Arce, V. B.; García, M. A.; *Food Hydrocolloids* **2017**, *70*, 152. [Crossref]
- Kumar, S.; Shukla, A.; Baul, P. P.; Mitra, A.; Halder, D.; *Food Packag. Shelf Life* **2018**, *16*, 178. [Crossref]
- Bindhu, M. R.; Umadevi, M.; Esmail, G. A.; Al-Dhabi, N. A.; Arasu, M. V.; *J. Photochem. Photobiol., B* **2020**, *205*, 111836. [Crossref]

18. Mohammadalinejad, S.; Almasi, H.; Esmaili, M.; *Mater. Sci. Eng., C* **2019**, *105*, 110115. [Crossref]
19. Rajeshkumar, S.; Bharath, L. V.; *Chem. Biol. Interact.* **2017**, *273*, 219. [Crossref]
20. K p, F.  .;  oşkunçay, S.; Duman, F.; *Mater. Sci. Eng., C* **2020**, *107*, 110207. [Crossref]
21. Valsalam, S.; Agastian, P.; Esmail, G. A.; Ghilan, A. K. M.; Al-Dhabi, N. A.; Arasu, M. V.; *J. Photochem. Photobiol., B* **2019**, *201*, 111670. [Crossref]
22. Asimuddin, M.; Shaik, M. R.; Adil, S. F.; Siddiqui, M. R. H.; Alwarthan, A.; Jamil, K.; Khan, M.; *J. King Saud Univ., Sci.* **2020**, *32*, 648. [Crossref]
23. Silveira, A. P.; Bonatto, C. C.; Lopes, C. A. P.; Rivera, L. M. R.; Silva, L. P.; *Mater. Chem. Phys.* **2018**, *216*, 476. [Crossref]
24. Espitia, P. J. P.; Soares, N. F. F.; Te filo, R. F.; Coimbra, J. S. R.; Vitor, D. M.; Batista, R. A.; Ferreira, S. O.; de Andrade, N. J.; Medeiros, E. A. A.; *Carbohydr. Polym.* **2013**, *94*, 199. [Crossref]
25. ASTM D883-12: *Standard Terminology Relating to Plastics*, Philadelphia, 2016.
26. ASTM E96/E96M: *Standard Test Methods for Water Vapor Transmission of Materials*, Philadelphia, 2015.
27. de Deus, T. B.; Barros, L. S. S.; da Silva, R. M.; Lima, W. K. S.; Lima, D. V.; Silva, A. S.; *Int. J. Microbiol.* **2017**, *2017*, ID 8173741. [Crossref]
28. Berlec, A.; Janež, N.; Sterniša, M.; Klan nik, A.; Sabotič, J.; *Front. Microbiol.* **2021**, *12*, 636421. [Crossref]
29. Saraiva, B. B.; Rodrigues, B. M.; da Silva Jr., R. C.; Scapim, M. R. S.; Lancheros, C. A. C.; Nakamura, C. V.; Caetano, W.; Pereira, P. C. S.; de Santana, E. H. W.; Pozza, M. S. S.; *LWT* **2021**, *151*, 112143. [Crossref]
30. Blum-Silva, C. H.; Luz, A. B. G.; Nascimento, M. V. P. S.; Facchin, B. M. C.; Baratto, B.; Fr de, T. S.; Sandjo, L. P.; Dalmarco, E. M.; Reginatto, F. H.; *Data Brief* **2016**, *8*, 295. [Crossref]
31. Filip, R.; Lotito, S. B.; Ferraro, G.; Fraga, C. G.; *Nutr. Res.* **2000**, *20*, 1437. [Crossref]
32. Bracesco, N.; Sanchez, A. G.; Contreras, V.; Menini, T.; Gugliucci, A.; *J. Ethnopharmacol.* **2011**, *136*, 378. [Crossref]
33. dos Santos, L. P.; Caon, T.; Battisti, M. A.; da Silva, C. H. B.; Sim es, C. M. O.; Reginatto, F. H.; de Campos, A. M.; *Ind. Crops Prod.* **2017**, *108*, 738. [Crossref]
34. Noguez, C.; *J. Phys. Chem. C* **2007**, *111*, 3806. [Crossref]
35. Alkhulaifi, M. M.; Alshehri, J. H.; Alwehaibi, M. A.; Awad, M. A.; Al-enazi, N. M.; Aldosari, N. S.; Hatamleh, A. A.; Raouf, N. A.; *Saudi J. Biol. Sci.* **2020**, *27*, 3434. [Crossref]
36. Tailor, G.; Yadav, B. L.; Chaudhary, J.; Joshi, M.; Suvalka, C.; *Biochem. Biophys. Rep.* **2020**, *24*, 100848. [Crossref]
37. Ponsanti, K.; Tangnorawich, B.; Ngernyuang, N.; Pechyen, C.; *J. Mater. Res. Technol.* **2020**, *9*, 11003. [Crossref]
38. Han, H.; Wang, H.; Gao, G.; Rao, P.; Zhou, J.; Ke, L.; Xu, Y.; *Food Control* **2022**, *133*, 108643. [Crossref]
39. Guo, C.; Chen, Y.; Li, J.; Zhan, F.; Wei, X.; Li, B.; *Food Chem.* **2021**, *339*, 128112. [Crossref]
40. Lin, X.; Chen, Z.; Zhang, Y.; Luo, W.; Tang, H.; Deng, B.; Deng, J.; Li, B.; *Food Chem.* **2015**, *173*, 432. [Crossref]
41. Rolim, W. R.; Pelegrino, M. T.; Lima, B. A.; Ferraz, L. S.; Costa, F. N.; Bernardes, J. S.; Rodrigues, T.; Brocchi, M.; Seabra, A. B.; *Appl. Surf. Sci.* **2019**, *463*, 66. [Crossref]
42. Umai, D.; Vikranth, A.; Meenambiga, S. S.; *Mater. Today: Proc.* **2021**, *44*, 3647. [Crossref]
43. Haider, M. J.; Mehdi, M. S.; *Int. J. Sci. Eng. Res.* **2014**, *5*, 381. [Link] accessed in August 2022
44. Teixeira, S. C.; Silva, R. R. A.; de Oliveira, T. V.; Stringheta, P. C.; Pinto, M. R. M. R.; Soares, N. F. F.; *Food Biosci.* **2021**, *42*, 101202. [Crossref]
45. Montero, B.; Rico, M.; Rodr guez-Illamazares, S.; Barral, L.; Bouza, R.; *Carbohydr. Polym.* **2017**, *157*, 1094. [Crossref]
46. Rahman, W. A. W. A.; Sin, L. T.; Rahmat, A. R.; Samad, A. A.; *Carbohydr. Polym.* **2010**, *81*, 805. [Crossref]
47. de Dicastillo, C. L.; Bustos, F.; Guarda, A.; Galotto, M. J.; *Food Hydrocolloids* **2016**, *60*, 335. [Crossref]
48. Estrada-Monje, A.; Zitzumbo-Guzm n, R.; Ba uelos-D az, J. A.; Zaragoza-Contreras, E. A.; *Mater. Chem. Phys.* **2019**, *235*, 121760. [Crossref]
49. Hong, S.-I.; Wang, L.-F.; Rhim, J.-W.; *Food Packag. Shelf Life* **2022**, *31*, 100784. [Crossref]
50. Roy, S.; Rhim, J.; *Food Biosci.* **2022**, *49*, 101867. [Crossref]
51. del Olmo, A.; Calzada, J.; Nu ez, M.; *Food Control* **2018**, *86*, 359. [Crossref]
52. Lewisoscar, F.; Nithya, C.; Vismaya, S.; Arunkumar, M.; Pugazhendhi, A.; Nguyen-Tri, P.; Alharbi, S. A.; Alharbi, N. F.; Thajuddin, N.; *Prog. Org. Coat.* **2021**, *151*, 106058. [Crossref]
53. Sarkar, R.; Kumar, C. A.; Kumbhakar, P.; Mandal, T.; *Mater. Today Proc.* **2019**, *11*, 686. [Crossref]

Submitted: April 11, 2022

Published online: August 30, 2022

